

# Calculate the CMB power spectrum: Cosmology II

Johan Mylius Kroken<sup>1,2</sup>

<sup>1</sup> Institute of Theoretical Astrophysics (ITA), University of Oslo, Norway

<sup>2</sup> Center for Computing in Science Education (CCSE), University of Oslo, Norway

April 12, 2023    GitHub repo link: <https://github.com/Johanmkr/AST5220/tree/main/project>

## ABSTRACT

SOME ABSTRACT

## Contents

### 1 Introduction

### 2 Milestone II - Recombination History

- 2.1 Theory . . . . .
  - 2.1.1 Hydrogen recombination . . . . .
  - 2.1.2 Visibility . . . . .
  - 2.1.3 Sound horizon . . . . .
- 2.2 Methods . . . . .
  - 2.2.1 Computing  $X_e$  . . . . .
  - 2.2.2 Computing  $\tau$  and  $\tilde{g}$  . . . . .
  - 2.2.3 Analysis . . . . .
- 2.3 Results and discussion . . . . .
  - 2.3.1 Times and sound horizon . . . . .
  - 2.3.2 Free electron fraction . . . . .
  - 2.3.3 Visibility . . . . .
  - 2.3.4 General discussion . . . . .

### 3 Milestone III - Perturbations

- 3.1 Theory . . . . .
  - 3.1.1 Metric perturbations . . . . .
  - 3.1.2 Fourier space and multipole expansion . . . . .
  - 3.1.3 Einstein-Boltzmann equations . . . . .
  - 3.1.4 Tight coupling regime . . . . .
  - 3.1.5 Inflation . . . . .
  - 3.1.6 Initial conditions . . . . .
- 3.2 Methods . . . . .
- 3.3 Results and discussion . . . . .

### A Useful derivations

- A.1 Angular diameter distance . . . . .
- A.2 Luminosity distance . . . . .
- A.3 Differential equations . . . . .

### B Sanity checks

- B.1 For  $\mathcal{H}$  . . . . .
- B.2 For  $\eta$  . . . . .

## Nomenclature

### 2 Constants of nature

- $m_e$  - Mass of electron.  
 $m_e = 9.10938356 \cdot 10^{-31}$  kg.
- $m_H$  - Mass of hydrogen atom.  
 $m_H = 1.6735575 \cdot 10^{-27}$  kg.
- $G$  - Gravitational constant.  
 $G = 6.67430 \cdot 10^{-11}$  m<sup>3</sup> kg<sup>-1</sup> s<sup>-2</sup>.
- $k_B$  - Boltzmann constant.  
 $k_B = 1.38064852 \cdot 10^{-23}$  m<sup>2</sup> kg s<sup>-2</sup> K<sup>-1</sup>.
- $\hbar$  - Reduced Planck constant.  
 $\hbar = 1.054571817 \cdot 10^{-34}$  J s<sup>-1</sup>.
- $c$  - Speed of light in vacuum.  
 $c = 2.99792458 \cdot 10^8$  m s<sup>-1</sup>.
- $\sigma_T$  - Thomson cross section.  
 $\sigma_T = 6.6524587158 \cdot 10^{-29}$  m<sup>2</sup>.
- $\alpha$  - Fine structure constant.  
 $\alpha = \frac{m_e c}{\hbar} \sqrt{\frac{3\sigma_T}{8\pi}}$

### 6 Cosmological parameters

- $G_{\mu\nu}$  - Einstein tensor.
- $T_{\mu\nu}$  - Stress-energy tensor.
- $H$  - Hubble parameter.
- $\mathcal{H}$  - Conformal Hubble parameter.
- $T_{\text{CMB0}}$  - Temperature of CMB today.
- $a$  - Scale factor.
- $x$  - Logarithm of scale factor.
- $t$  - Cosmic time.
- $z$  - Redshift.
- $\eta$  - Conformal time.
- $\chi$  - Co-moving distance.
- $p$  - Pressure.
- $\rho$  - Density.
- $r$  - Radial distance.
- $d_A$  - Angular diameter distance.
- $d_L$  - Luminosity distance.
- $n_e$  - Electron density.
- $n_b$  - Baryon density.
- $X_e$  - Free electron fraction.
- $\tau$  - Optical depth.
- $\tilde{g}$  - Visibility function.
- $s$  - Sound horizon.
- $r_s$  - Sound horizon at decoupling.
- $c_s$  - Wave propagation speed.

### Density parameters

Density parameter  $\Omega_X = \rho_X/\rho_c$  where  $\rho_X$  is the density and  $\rho_c = 8\pi G/3H^2$  the critical density.  $X$  can take the following values:

- $b$  - Baryons.
- CDM - Cold dark matter.
- $\gamma$  - Electromagnetic radiation.
- $\nu$  - Neutrinos.
- $k$  - Spatial curvature.
- $\Lambda$  - Cosmological constant.

A 0 in the subscript indicates the present day value.

### Fiducial cosmology

The fiducial cosmology used throughout this project is based on the observational data obtained by [Aghanim et al. \(2020\)](#):

$$\begin{aligned}
 h &= 0.67, \\
 T_{\text{CMB}0} &= 2.7255 \text{ K}, \\
 N_{\text{eff}} &= 3.046, \\
 \Omega_{b0} &= 0.05, \\
 \Omega_{\text{CDM}0} &= 0.267, \\
 \Omega_{k0} &= 0, \\
 \Omega_{\nu0} &= N_{\text{eff}} \cdot \frac{7}{8} \left( \frac{4}{11} \right)^{4/3} \Omega_{\gamma0}, \\
 \Omega_{\Lambda0} &= 1 - (\Omega_{k0} + \Omega_{b0} + \Omega_{\text{CDM}0} + \Omega_{\gamma0} + \Omega_{\nu0}), \\
 \Omega_{M0} &= \Omega_{b0} + \Omega_{\text{CDM}0}, \\
 \Omega_{\text{rad}} &= \Omega_{\gamma0} + \Omega_{\nu0}, \\
 n_s &= 0.965, \\
 A_s &= 2.1 \cdot 10^{-9}.
 \end{aligned}$$

## 1. Introduction

Introduce all for Milestones and the overall aim of calculating the CMB power spectrum etc.

**TODO: Obviously this introduction will change and amended as more milestones are completed.**

## 2. Milestone II - Recombination History

The main goal of this section is to investigate the recombination history of the universe. This can be explained as the point in time when photons decouple from the equilibrium of the opaque, early universe. When this happens, photons scatter for the last time at the *time of last scattering*, and these photons are what we today observe as the CMB. This period of the history of the universe is thus crucial for understanding the CMB.

We will start by calculating the free electron fraction  $X_e$ , from which we may find the optical depth  $\tau$ . This again enables us to compute the visibility function,  $g$ , and the sound horizon,  $s$ . The latter will be of great importance later.

Recombination happens because the expansion of the Universe cools it down, making the photons less energetic, which in turn make each interaction in the primordial plasma less energetic. At some point, hydrogen atoms are

able to form, reducing the number of free electron, hence reducing photon interactions, until they scatter for the last time. We will determine the time of recombination from the free electron fraction, which indirectly tell us how large portion of the free electron have (re)-combined.<sup>1</sup> Due to the decrease of free electron, photons interact less with them (optical depth is decreased). At some point, photons scatter for the last time, and this information is encapsulated in the visibility function.

### 2.1. Theory

In order to explain the inventory of the universe, we need to understand how the distribution of different species changes over time. This is governed by the *Boltzmann equation*,

$$\frac{df}{dt} = C[f], \quad (1)$$

where  $f(\mathbf{r}, \mathbf{p}, t)$ <sup>2</sup> is the distribution function of a given species.  $C[f]$  are the collision terms, which depends on the species through the same distribution function  $f$ . Due to the function dependencies of  $f$  the general collision terms are expanded into ([Dodelson & Schmidt \(2020\)](#)):

$$C[f] = \frac{\partial f}{\partial t} + \frac{\partial f}{\partial x^i} \frac{dx^i}{dt} + \frac{\partial f}{\partial p} \frac{dp}{dt} + \frac{\partial f}{\partial \hat{p}^i} \frac{d\hat{p}^i}{dt}, \quad (2)$$

where  $p = |\mathbf{p}|$  and  $\hat{p} = \mathbf{p}/p$ .

Before recombination, the equilibrium between protons, electrons and photons is governed by the following interaction, from [Weinberg \(2008\)](#)<sup>3</sup>:

$$e^- + p^+ \rightleftharpoons H^* + \gamma, \quad (3)$$

where a proton and an electron interact to form an excited hydrogen atom, which decays and emits a photon, or a photon excites and split a hydrogen atom into a free electron and a proton through *Compton scattering*.<sup>4</sup> Eq. (3) is a reaction of the form  $1 + 2 \rightleftharpoons 3 + 4$ , and we have from [Winther et al. \(2023\)](#) that the Boltzmann equation for such a reaction is:

$$\frac{1}{n_1 e^{3x}} \frac{d(n_1 e^{3x})}{dx} = -\frac{\Gamma}{H} \left( 1 - \frac{n_3 n_4}{n_1 n_2} \left( \frac{n_1 n_2}{n_3 n_4} \right)_{\text{eq}} \right), \quad (4)$$

where  $n_i$  are the number densities of the reactants,  $\Gamma$  is the reaction rate and  $H$  the Hubble parameter (expansion rate of the universe). If the reaction rate is much larger than

<sup>1</sup> As with any good article on the subject, we ought to say that recombination is a funny wording, as this is the first time in the history of the Universe that protons and electrons combine to form hydrogen.

<sup>2</sup> Given in *phase-space coordinates*:  $(x^\mu, P^\mu)$

<sup>3</sup> Where  $H^*$  denotes excited states of hydrogen which will decay into neutral hydrogen.

<sup>4</sup> Elastic scattering of photons is technically Thomson scattering, but Compton scattering is a more general term and will be used ([Dodelson & Schmidt \(2020\)](#)). This is also why we later use the Thomson cross section  $\sigma_T$ . The reaction is when a photon scatters of an electron, and possibly energises it enough to break out of the hydrogen atom, if already bound:

$$\gamma + e^- \rightleftharpoons \gamma + e^-.$$

the expansion rate of the universe,  $\Gamma \gg H$ , then Eq. (3) ensures equilibrium between protons, electron and photons. When  $\Gamma$  drops below  $H$ , then the expansion rate becomes dominant and the reaction rate is unable to sustain equilibrium. This happens when the temperature of the Universe becomes lower than the binding energy of hydrogen, hence stable neutral hydrogen is able to form.<sup>5</sup> As a consequence, the photons *decouple* from the protons and electron. When  $\Gamma \ll H$ , there are practically no interactions and the number density becomes constant for a comoving volume. Massive particles *freeze out* and their abundance become constant.

### 2.1.1. Hydrogen recombination

We express the electron density through the free electron fraction  $X_e \equiv n_e/n_H = n_e/n_b$  where we have assumed that hydrogen make up all the baryons ( $n_b = n_H$ ). We also ignore the difference between free protons and neutral hydrogen. From Callin (2006) we obtain:

$$n_b = \frac{\rho_b}{m_H} = \frac{\Omega_b \rho_c}{m_H} e^{-3x}, \quad (5)$$

where  $m_H$  is the mass of the hydrogen atom, and  $\rho_c$  the critical density today as defined earlier. Before recombination, no stable neutral hydrogen is formed, thus the electron and baryon density is the same, i.e. there are only free electrons so  $X_e \simeq 1$ . When in equilibrium, the r.h.s. of Eq. (4) reduces to 0, which is called the *Saha approximation*. The solution is in this regime described by the *Saha equation*, which from Dodelson & Schmidt (2020) in physical units is:

$$\frac{X_e^2}{1 - X_e} = \frac{1}{n_b} \left( \frac{k_B m_e T_b}{2\pi \hbar^2} \right)^{3/2} e^{-\epsilon_0/k_B T_b}, \quad (6)$$

where  $\epsilon_0 = 13.6$  eV is the ionisation energy of hydrogen. The Saha equation is only a good approximation when  $X_e \simeq 1$ . Thus for  $X_e < (1 - \xi)$ ,<sup>6</sup> which corresponds to the period during and after recombination, we have to make use of the more accurate *Peebles equation*. From Callin (2006):

$$\frac{dX_e}{dx} = \frac{C_r(T_b)}{H} \left[ \beta(T_b)(1 - X_e) - n_H \alpha^{(2)}(T_b) X_e^2 \right], \quad (7)$$

<sup>5</sup> Well, it is really not as simple, as neutral hydrogen is obtained from excited hydrogen and how this process go about is non-trivial. As we ignore re-ionisation, I will not delve into this. However, both (Weinberg 2008, p. 113-129), (Dodelson & Schmidt 2020, p. 95-99) and Winther et al. (2023) elaborate further on this.

<sup>6</sup> Where  $\xi$  is some small tolerance, which have to be defined in some numerical model for when to abandon the Saha equation and use the more accurate, but computationally more expensive Peebles equation. This is typically  $\xi = 0.001$

where

$$C_r(T_b) = \frac{\Lambda_{2s-1s} + \Lambda_\alpha}{\Lambda_{2s-1s} + \Lambda_\alpha + \beta^{(2)}(T_b)}, \quad (7a)$$

$$\Lambda_{2s-1s} = 8.227 \text{ s}^{-1}, \quad (7b)$$

$$\Lambda_\alpha = \frac{1}{(\hbar c)^3} H \frac{(3\epsilon_0)^3}{(8\pi)^2 n_{1s}}, \quad (7c)$$

$$n_{1s} = (1 - X_e) n_H, \quad (7d)$$

$$n_H = (1 - Y_p) \frac{3H_0^2 \Omega_{b0}}{8\pi G m_H} e^{-3x}, \quad (7e)$$

$$\beta^{(2)}(T_b) = \beta(T_b) e^{3\epsilon_0/4k_B T_b}, \quad (7f)$$

$$\beta(T_b) = \alpha^{(2)}(T_b) \left( \frac{k_B m_e T_b}{2\pi \hbar^2} \right)^{3/2} e^{-\epsilon_0/k_B T_b}, \quad (7g)$$

$$\alpha^{(2)}(T_b) = \frac{\hbar^2}{c} \frac{64\pi}{\sqrt{27}\pi} \frac{\alpha^2}{m_e^2} \sqrt{\frac{\epsilon_0}{k_B T_b}} \phi_2(T_b), \quad (7h)$$

$$\phi_2(T_b) = 0.448 \ln \left( \frac{\epsilon_0}{k_B T_b} \right). \quad (7i)$$

The Peebles equation takes into account that the energy (excitation) of hydrogen formed through Eq. (3) vary, and that decays take place until we reach the  $n = 2$  level (first excited state), denoted by <sup>(2)</sup> in Eq. (7a)- Eq. (7i). Recombination to the ground state is not relevant, as this leads to an ionised photon which immediately ionises a neutral hydrogen atom (Dodelson & Schmidt 2020, p. 97). The  $C_r$  is the probability that singly ionised hydrogen is reionised further, where  $\beta^{(2)}$  and  $\beta$  are the collisional ionisations from the first ionised state and ground state respectively.  $\alpha^{(2)}$  is the recombination rate to excited states. For more detailed description of these terms, see Ma & Bertschinger (1995).<sup>7</sup>

We find  $X_e$  by solving Eq. (6) for  $X_e > (1 - \xi)$  and Eq. (7) for  $X_e < (1 - \xi)$ . In theory, it is possible to solve the Peebles equation at very early times, but the equation is very stiff resulting in unstable numerical solutions at early times (high temperatures), hence the Saha approximation.

### 2.1.2. Visibility

Visibility is a concept tied to the optical depth and mean free path of a medium. The two latter are inversely proportional to each other. The mean free path is the average distance a photon travels before its direction is changed (often by scattering). Thus, a small mean free path gives results in a lot of collision across short distances, which occurs in optically thick media. The optical depth as a function of conformal time is defined as Winther et al. (2023):

$$\tau = \int_\eta^{\eta_0} n_e \sigma_T e^{-x} d\eta', \quad (8)$$

where  $n_e$  is the electron density and  $\sigma_T$  is the Thompson cross-section. In differential form, restoring original units, this is:

$$\frac{d\tau}{dx} = - \frac{c n_e \sigma_T e^x}{\mathcal{H}}. \quad (9)$$

<sup>7</sup> Because of this non-trivial path into the ground state, and the large photon to baryon number ratio, recombination happens later than when the temperature of the universe correspond to exactly the binding energy of neutral hydrogen (Callin (2006))

From this we define the visibility function,  $g$ :

$$g = -\frac{d\tau}{d\eta}e^{-\tau} = -\mathcal{H}\frac{d\tau}{dx}e^{-\tau}$$

$$\tilde{g} \equiv -\frac{d\tau}{dx}e^{-\tau} = \frac{g}{\mathcal{H}}, \quad (10)$$

where  $\tilde{g}$  is in terms of the preferred time variable,  $x$ . Notable thing about the visibility function  $\tilde{g}$  is that it is a true probability distribution, describing the probability density of some photon to last have been scattered at time  $x$ . Because of this, we have that  $\int_{-\infty}^0 \tilde{g}(x)dx = 1$ . We also take note of the derivative of the visibility function:

$$\frac{d\tilde{g}}{dx} = e^{-\tau} \left[ \left( \frac{d\tau}{dx} \right)^2 - \frac{d^2\tau}{dx^2} \right] \quad (11)$$

### 2.1.3. Sound horizon

Let's take a small step back and consider the situation of the early Universe. Before any decoupling, the photons and electrons are coupled through Thompson scattering, and protons and electrons are coupled through coulomb interactions. Because of this, photons interact with baryons and move alongside with them as one fluid, in which wave propagates with a speed  $c_s$ , from [Dodelson & Schmidt \(2020\)](#):

$$c_s \equiv c [3(1+R)]^{-\frac{1}{2}} \quad ; \quad R \equiv \frac{3\Omega_b}{4\Omega_\gamma}, \quad (12)$$

where  $R$  is the *baryon-to-photon energy ratio*. By the definition of  $R$ , if the baryon density is negligible compared to the radiation density,  $R \sim 0$ , and we recover the wave propagation speed in a relativistic fluid:  $c_s = 3^{-1/2}$  ([Dodelson & Schmidt \(2020\)](#)). The total distance such a wave would have travelled in a time  $t$  (since the beginning of the Universe) is called the *sound horizon*, found by simply integrating  $c_s$  through time, accounting for the expansion of space itself by including a factor  $e^{-x}$ :

$$s = \int_0^t c_s e^{-x} dt = \int_{-\infty}^x \frac{c_s}{\mathcal{H}} dx, \quad (13)$$

where the variables are changed to  $x$ . On differential form:

$$\frac{ds}{dx} = \frac{c_s}{\mathcal{H}}, \quad (14)$$

which is a straightforward differential equation to solve given some initial conditions.

## 2.2. Methods

### 2.2.1. Computing $X_e$

First things first, we need to compute the free electron fraction  $X_e$ . We are for the most part not interested in things happening in the future here, so the temporal range of choice will be  $x \in [-20, 0)$  where  $x = 0$  is today, and  $x = -20$  is sufficiently long ago, so that the range encapsulated effect studied here. In the early Universe, the energies are so high that all baryonic matter is in the form of free electron,  $X_e \simeq 1$ , so we will start by solving the Saha equation, Eq. (6). We continue to solve equation Eq. (6) as long as  $X_e > 1 - \xi$  where we use  $\xi = 0.01$ .

If we define:

$$K \equiv \frac{1}{n_b} \left( \frac{k_B m_e T_b}{2\pi\hbar^2} \right)^{3/2} e^{-\epsilon_0/k_B T_b}, \quad (15)$$

then equation Eq. (6) takes the form  $X_e^2 + KX_e - K = 0$ , which is solved as a normal quadratic equation<sup>8</sup>, where  $a = 1$ ,  $b = K$  and  $c = -K$ . Since  $0 \leq X_e \leq 1$  we choose the positive solution, given by:

$$X_e = \frac{-K + \sqrt{K^2 + 4K}}{2} = \frac{K}{2} \left( -1 + \sqrt{1 + 4K^{-1}} \right) \quad (16)$$

This solution has the potential to become numerically unstable if the parenthesis is close to zero, i.e. for  $K \gg 1$ . We then make use of the approximation  $\sqrt{1 + 4K^{-1}} \approx 1 + (2K^{-1})$  for  $|4K^{-1}| \ll 1$ , which ensures  $X_e \simeq 1$  for very high temperatures (large  $K$ ).

We continue to solve the Peebles equation as stated in Eq. (7), where the r.h.s. is implemented sequentially as Eq. (7a)- Eq. (7i) in reverse order. The initial condition is the last computed electron fraction above the cut-off:  $X_{e0} = \min(X_e > 1 - \xi)$  as found from the Saha equation. It is solved for the x-range not solved by the Saha equation. On thing to notice is that for late time,  $T_b$  becomes small, meaning that  $e^{\epsilon_0/k_B T_b}$  becomes enormous. This term is found in Eq. (7f), and we solve it by setting  $\beta^{(2)}(T_b) = 2$  if  $\epsilon/k_B T_b > 200$ , in order to avoid overflow.

Having found  $X_e$  for the entire x-range, we compute  $n_e$  and spline both results.

### 2.2.2. Computing $\tau$ and $\tilde{g}$

With  $n_e$  we are able to solve the optical depth as defined in Eq. (9). The initial condition for this equation is that the optical depth today is zero:  $\tau(x = 0) = 0$ , meaning we have to solve this backwards in time. This is done by using the negative differential:

$$\frac{d\tau_{\text{rev}}}{dx_{\text{rev}}} = -\frac{d\tau}{dx} = \frac{cn_e\sigma_T e^x}{\mathcal{H}}, \quad (17)$$

and solving for positive  $x_{\text{rev}}$ :  $x_{\text{rev}} \in [0, 20]$ . In order to undo this reversal, we map  $\tau = -\tau_{\text{rev}}$  to its corresponding  $x = -x_{\text{rev}}$ . Having found  $\tau$ , we find its derivative by solving equation Eq. (9), and further the find the visibility function from Eq. (10) and its derivative from Eq. (11). We ensure that  $\int_{-\infty}^0 \tilde{g}dx = 1$  as a sanity check. All of these four quantities are splined, and their derivatives are obtained numerically.

In order to solve equation Eq. (13) for the sound horizon, we choose initial conditions  $s_i = c_{s,i}/\mathcal{H}_i$  where the subscript  $i$  denote a very early time (in our case when  $x = -20$ ). We are then able to solve the differential equation for the sound horizon, Eq. (14), numerically and then spline the result.

<sup>8</sup>  $ay^2 + by + c = 0$  has solutions

$$y = \frac{-b \pm \sqrt{b^2 - 4ac}}{2}.$$



Phenomenon	$x$	$z$	$t$ [Myr]	$r_s$ [Mpc]
Last scattering	-6.9853	1079.67	0.3780	145.31
Recombination	-6.9855	1079.83	0.3779	145.29
Saha	-7.1404	1260.89	0.2909	131.03

**Table 1.** The times of last scattering and recombination given in terms of  $x$ , the redshift  $z$ , the cosmic time  $t$  and the sound horizon  $r_s$ . Also included is the time of recombination found using the Saha approximation only.

### 2.2.3. Analysis

Having splines for the relevant quantities enables us to compute some important times in the early universe. Firstly, the *last scattering surface*, is the time when most photons scattered for the last time, and decoupled from the plasma. This is not expected to have happened instantly, but recalling that the visibility function  $\tilde{g}$  is a probability distribution function for when photons last scattered, we simply use the peak of this function as the definition of the last scattering surface.

Further, we want to find a time for when recombination happened, i.e. when free electron was captured by protons to form hydrogen atoms. Thus, this coincides with the reduction of the free electron fraction, and we will use  $X_e = 0.1$  as the definition for when recombination happened. These numbers can also be computed using only the Saha approximation, for comparison. We also compute the sound horizon at these decouplings:  $r_s = s(x_{\text{dec}})$ .

The last thing we want to compute is the freeze out abundance of free electrons, i.e. the free electron abundance today, which is found by evaluating the spline for  $X_e$  at  $x = 0$ .

## 2.3. Results and discussion

### 2.3.1. Times and sound horizon

The relevant times for last scattering, recombination and Saha recombination are obtained as explained in Section 2.2.3, and presented in Section 2.3.1. These times are given in terms of  $x$ , the redshift  $z$  and the cosmic time  $t$  (in Myr). The sound horizon is given in units of megaparsecs (Mpc). Last scattering occurred when  $x = -6.9853$ , at redshift  $z = 1079.67$ , which is slightly after recombination when  $x = -6.9855$  at redshift  $z = 1079.83$ . If the Saha approximation was valid when the electron fraction dropped, recombination would have happened when  $x = -7.1404$  at redshift 1260.89 which is significantly earlier. However, this is not the case since photons drop out of equilibrium with the primordial plasma as soon as hydrogen begin to form, and the free electron fraction is reduced. Thus, this number may only be used for comparison. Another thing worth noting is the validity of these numbers.

### 2.3.2. Free electron fraction

Fig. 1 shows the free electron fraction  $X_e$  as a function of  $x$  found using both the Saha and Peebles equation, as explained in Section 2.2.1, in blue. Also shown is the results found from the Saha equation only, which tends to zero a lot faster. This is used for comparison only, as we have already stated that the Saha approximation is only valid for

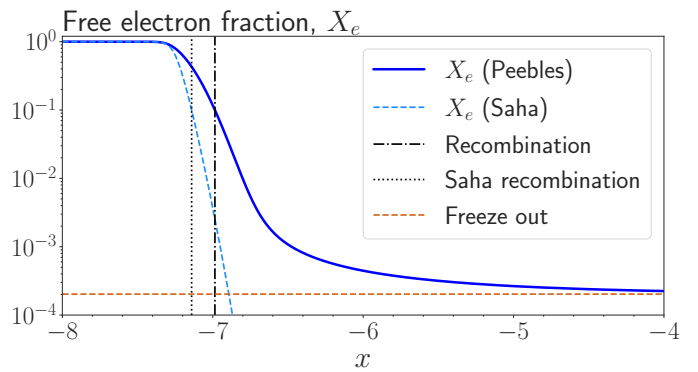


**Fig. 1.** The free electron fraction  $X_e$  as function of  $x$ , found from the Saha and Peebles equation (blue). The result using only the Saha equation is shown in dashed light blue. The time of recombination is shown as a dashed black line. Likewise, recombination in the Saha approximation is shown as a dotted black line, appearing earlier. The freeze out abundance of hydrogen (the present value) is shown as a brown dashed line.

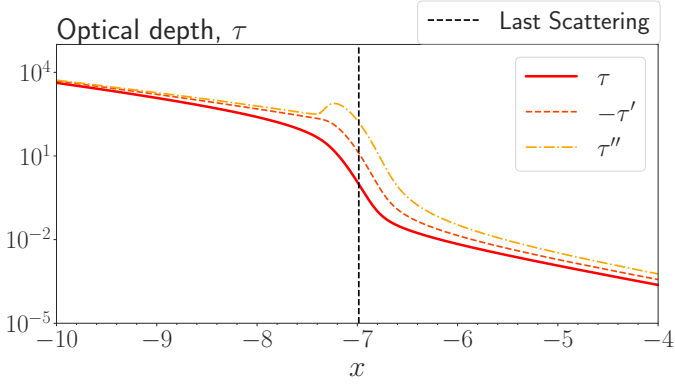
$X_e \simeq 1$ . The time of recombination is shown for both cases, which for the Saha approximation happens significantly earlier than what is the actual case. The Peebles solution falls off gradually, and converges towards a constant value, which is the present day abundance of free electrons (freeze out abundance). This is found to be  $X_e(x = 0) = 0.0002$ , shown as a brown dashed line in Fig. 1.

Since the Peebles equation is a solution of the Boltzmann equation, it takes into account the particle interaction with changing abundance, after the photons decouple from the primordial plasma. It is thus expected that this will result in a much more gradual fall off of the free electron fraction, just as we observe in Fig. 1.

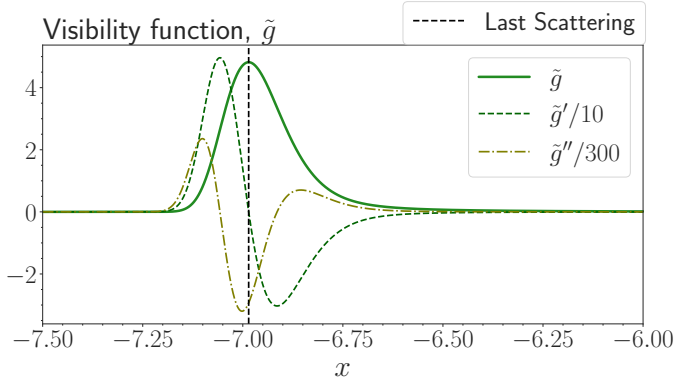
### 2.3.3. Visibility

Fig. 2 shows the optical depth and its first two derivatives as functions of  $x$ . The surface of last scattering is shown with a black dashed line, before which the primordial plasma is optically thick, meaning the photons have a short mean free path. The decrease of the optical depth means that the photons gradually travel longer distances before interacting with free electrons. There are two processes going on here; the expansion of space itself, and the formation of neutral hydrogen. Both of which contribute to the increased mean free path of the photons. The contribution from the expansion of space is slow compared to the seemingly rapid change in the free electron fraction once neutral hydrogen is able to form. Thus, the rapid decrease of free electrons, as seen in Fig. 1 makes the mean free paths of photon to increase beyond the horizon. This effectively enable them to travel through space without interacting with matter, and this is what we observe as the CMB today - the Universe becomes transparent. This sudden decrease of optical depth is clearly seen in Fig. 2, both in  $\tau$  itself, but also in its derivatives.

Another way of arriving at similar conclusions is by considering the visibility function in Fig. 3. Here,  $\tilde{g}$  is shown in green along with its derivatives. The scaling follow that of Callin (2006), in order to fit the graphs into the same figure.  $\tilde{g}$  describes the probability that a photon reaching us today scattered at time  $x$ . The peak of this function indi-



**Fig. 2.** The optical depth  $\tau$  and its first and second derivatives as functions of  $x$ . The time of last scattering is shown as a dashed black line, before which the Universe was optically thick.



**Fig. 3.** The visibility function  $\tilde{g}$  and its first and second derivatives as functions of  $x$ . The time of last scattering is shown as a dashed black line, which by definition coincides with the peak of the visibility function.

cates the time were *the most* photons scattered for the last time, and is thus used as a definition of the last scattering surface. The visibility function is skewed forward in time. **TODO: why?**

### 2.3.4. General discussion

One key thing to keep in mind is that recombination did not happen instantaneously, but rather over a relatively short period in which neutral hydrogen formed rapidly. This caused a rapid decrease of the free electron fraction, which again caused the optical depth to decrease by several magnitudes. In the same period, we see that the visibility function is non-zero, meaning the probability of last scattering is (relatively) very high in this period. The times quoted in Section 2.3.1 are times that arise from our quite rigid, but fair definition of last scattering and recombination. However, these times do not encapsulate the duration of the abovementioned period. One could also define the last scattering surface as the time when  $\tau = 1$  which is the transition between optically thick and optically thin media (when the photon travels exactly one mean free path before scattering). However, the visibility function is arguably a better choice since this is a proper probability distribution, so its peak represents the *actual* time when the probability of last scattering was the highest. Nevertheless, if we

change these definitions we ought to expect different times as a result.

## 3. Milestone III - Perturbations

The aim of this section is to investigate how small fluctuations in the baryon-photon-dark-matter fluid in the early grew into larger structures. This is done by examining the interplay between these fluid fluctuations and the subsequent fluctuations of the space-time geometry. We will model this by perturbing the flat FLRW-metric using the conformal-Newtonian gauge. This will impact how the Boltzmann equations for the different species behaves, from which we are able to construct differential equations for key physical observables, and their initial conditions.

### 3.1. Theory

#### 3.1.1. Metric perturbations

The perturbed metric in the conformal-Newtonian gauge is given in Callin (2006) as:

$$g_{\mu\nu} = \begin{pmatrix} -(1+2\Psi) & 0 \\ 0 & e^{2x}\delta_{ij}(1+2\Phi) \end{pmatrix} \quad (18)$$

#### 3.1.2. Fourier space and multipole expansion

Consider a function  $f(\mathbf{x}, t)$ . Its Fourier transform  $\mathcal{F}$  and inverse  $\mathcal{F}^{-1}$  are defined as:

$$\mathcal{F}[f(\mathbf{x}, t)] \equiv \frac{1}{(2\pi)^{3/2}} \int e^{-i\mathbf{k}\cdot\mathbf{x}} f(\mathbf{x}, t) d^3x = \tilde{f}(\mathbf{k}, t), \quad (19)$$

$$\mathcal{F}^{-1}[\tilde{f}(\mathbf{k}, t)] \equiv \frac{1}{(2\pi)^{3/2}} \int e^{i\mathbf{k}\cdot\mathbf{x}} \tilde{f}(\mathbf{k}, t) d^3k = f(\mathbf{x}, t). \quad (20)$$

It becomes apparent from these definitions that taking the spatial derivative with respect to  $\mathbf{x}$  in real space, is the same as multiplying the function with  $i\mathbf{k}$  in Fourier space. This leads to the following property:  $\mathcal{F}[\nabla f(\mathbf{x}, t)] = i\mathbf{k}\mathcal{F}[f(\mathbf{x}, t)]$ . This is of major significance when working with partial differential equations (PDEs), where:

$$\begin{aligned} \mathcal{F}[\nabla^2 f(\mathbf{x}, t)] &= i^2 \mathbf{k} \cdot \mathbf{k} \mathcal{F}[f(\mathbf{x}, t)] = -k^2 \mathcal{F}[f(\mathbf{x}, t)] \\ \mathcal{F}\left[\frac{d^n f(\mathbf{x}, t)}{dt^n}\right] &= \frac{d^n}{dt^n} \mathcal{F}[f(\mathbf{x}, t)]. \end{aligned} \quad (21)$$

The two equations in Eq. (21) have the ability of reducing PDEs down to a set of decoupled ODEs. This means that we are able to solve for each mode  $k = |\mathbf{k}|$  independently, which will be of great impact for the equations to come.

We will also work with multipole expansions, which are series written as sums of *Legendre polynomials* expanded in  $\mu = \cos \theta \in [-1, 1]$  as:

$$f(\mu) = \sum_{l=0}^{\infty} f_l \mathcal{P}_l(\mu), \quad (22)$$

where  $\mathcal{P}_l$  is the  $l$ -th Legendre polynomial. These are orthogonal in such a way that they form a complete basis, enabling us to express any  $f(\mu)$  as in Eq. (22). The coefficients  $f_l$  are the *Legendre multipoles*:

$$f_l = \frac{2l+1}{2} \int_{-1}^1 f(\mu) \mathcal{P}_l(\mu) d\mu. \quad (23)$$

### 3.1.3. Einstein-Boltzmann equations

The conformal-Newtonian gauge perturbation, Eq. (18), give rise to the Boltzmann equation for radiation and massive particles, both found from the general Boltzmann equation in Eq. (4). We now solve the Boltzmann equation for the different species, starting with photons. In linear order, we have from (Dodelson & Schmidt 2020, Eq. 3.74) that:

$$\frac{df}{dt} = \frac{\partial f}{\partial t} + \frac{\hat{p}^i}{a} \frac{\partial f}{\partial x^i} - \left[ H + \dot{\Phi} + \frac{1}{a} \hat{p}^i \frac{\partial \Psi}{\partial x^i} \right] p \frac{\partial f}{\partial p}. \quad (24)$$

We then define the perturbation to the photons,  $\Theta$ , to be the variation of photon temperature around an equilibrium temperature  $T^{(0)}$ :

$$T(\mathbf{x}, \mathbf{p}, t) = T^{(0)} [1 + \Theta(\mathbf{x}, \mathbf{p}, t)]. \quad (25)$$

The collision terms for the photons are governed by Compton scattering **TODO: decide on how much to include here** By expanding equation Eq. (24) around its zeroth order Bose-Einstein form (Dodelson & Schmidt (2020)), using the temperature perturbation in Eq. (25) we obtain the following:

$$\dot{\Theta} + \frac{\hat{p}^i}{a} \frac{\partial \Theta}{\partial x^i} + \dot{\Phi} + \frac{\hat{p}^i}{a} \frac{\partial \Psi}{\partial x^i} = n_e \sigma_T [\Theta_0 - \Theta + \hat{\mathbf{p}} \cdot \mathbf{v}_b] \quad (26)$$

from (Dodelson & Schmidt 2020, Eq. 3.76):

$$\frac{df}{dt} = \frac{\partial f}{\partial t} + \frac{p}{E} \frac{\hat{p}^i}{a} \frac{\partial f}{\partial x^i} - \left[ H + \dot{\Psi} + \frac{E}{ap} \hat{p}^i \Psi_i \right] p \frac{\partial f}{\partial p} \quad (27)$$

$$\dot{\Theta} = -ik\mu(\Theta + \Psi) - \dot{\Phi} - \dot{\tau} \left[ \Theta_0 - \Theta + i\mu v_b - \frac{\mathcal{P}_2 \Theta_2}{2} \right], \quad (28a)$$

$$\dot{\delta}_{\text{CDM}} = -3\dot{\Phi} + kv_{\text{CDM}} \quad (28b)$$

$$\dot{v}_{\text{CDM}} = -k\Psi - \mathcal{H}v_{\text{CDM}} \quad (28c)$$

$$(28d)$$

Photon temperature multipoles

$$\Theta'_0 = -\frac{ck}{\mathcal{H}} \Theta_1 - \Phi', \quad (29a)$$

$$\Theta'_1 = \frac{ck}{3\mathcal{H}} \Theta_0 - \frac{2ck}{3\mathcal{H}} \Theta_2 + \frac{ck}{3\mathcal{H}} \Psi + \tau' \left[ \Theta_1 + \frac{1}{3} v_b \right], \quad (29b)$$

$$\Theta_l = \begin{cases} \frac{lck\Theta_{l-1}}{(2l+1)\mathcal{H}} - \frac{(l+1)ck\Theta_{l+1}}{(2l+1)\mathcal{H}} + \tau' \left[ \Theta_l - \frac{\Theta_2}{10} \delta_{l,2} \right], & l \geq 2 \\ \frac{ck\Theta_{l-1}}{\mathcal{H}} - c \frac{(l+1)\Theta_l}{\mathcal{H}\eta} + \tau' \Theta_l, & l = l_{\text{max}} \end{cases} \quad (29c)$$

Cold dark matter and baryons

$$\delta'_{\text{CDM}} = \frac{ck}{\mathcal{H}} v_{\text{CDM}} - 3\Phi', \quad (30a)$$

$$v'_{\text{CDM}} = -v_{\text{CDM}} - \frac{ck}{\mathcal{H}} \Psi, \quad (30b)$$

$$\delta'_b = \frac{ck}{\mathcal{H}} v_b - 3\Phi', \quad (30c)$$

$$v'_b = -v_b - \frac{ck}{\mathcal{H}} + \tau' R^{-1} (3\Theta_1 + v_b) \quad (30d)$$

where  $R$  is defined in Eq. (12)

### Metric perturbations

$$\Phi' = \Psi - \frac{c^2 k^2}{3\mathcal{H}^2} \Phi + \frac{H_0^2}{2\mathcal{H}^2} \mathcal{Y}, \quad (31a)$$

$$\Psi = -\Phi - \frac{12H_0^2}{c^2 k^2} \Omega_\gamma \Theta_2. \quad (31b)$$

where  $\mathcal{Y} = \Omega_{\text{CDM}} \delta_{\text{CDM}} + \Omega_b \delta_b + 4\Omega_\gamma \Theta_0$

### 3.1.4. Tight coupling regime

### 3.1.5. Inflation

### 3.1.6. Initial conditions

### 3.2. Methods

some methods

### 3.3. Results and discussion

## References

- Aghanim, N., Akrami, Y., Ashdown, M., et al. 2020, *Astronomy & Astrophysics*, 641, A6
- Callin, P. 2006, *How to calculate the CMB spectrum*
- Dodelson, S. & Schmidt, F. 2020, *Modern Cosmology* (Elsevier Science)
- Ma, C.-P. & Bertschinger, E. 1995, *The Astrophysical Journal*, 455, 7
- Weinberg, S. 2008, *Cosmology*, Cosmology (OUP Oxford)
- Winther, H. A., Eriksen, H. K., Elgaroy, O., Mota, D. F., & Ihle, H. 2023, *Cosmology II*, <https://cmb.wintherscoming.no/>, accessed on March 1, 2023

## Appendix A: Useful derivations

### A.1. Angular diameter distance

This is related to the physical distance of say, an object, whose extent is small compared to the distance at which we observe is. If the extension of the object is  $\Delta s$ , and we measure an angular size of  $\Delta\theta$ , then the angular distance to the object is:

$$d_A = \frac{\Delta s}{\Delta\theta} = \frac{ds}{d\theta} = \sqrt{e^{2x} r^2} = e^x r, \quad (\text{A.1})$$

where we inserted for the line element  $ds$  as given in equation ??, and used the fact that  $dt/d\theta = dr/d\theta = d\phi/d\theta = 0$  in polar coordinates.

### A.2. Luminosity distance

If the intrinsic luminosity,  $L$  of an object is known, we can calculate the flux as:  $F = L/(4\pi d_L^2)$ , where  $d_L$  is the luminosity distance. It is a measure of how much the light has dimmed when travelling from the source to the observer. For further analysis we observe that the luminosity of objects moving away from us is changing by a factor  $a^{-4}$  due to the energy loss of electromagnetic radiation, and the observed flux is changed by a factor  $1/(4\pi d_A^2)$ . From this we draw the conclusion that the luminosity distance may be written as:

$$d_L = \sqrt{\frac{L}{4\pi F}} = \sqrt{\frac{d_A^2}{a^4}} = e^{-x} r \quad (\text{A.2})$$

### A.3. Differential equations

From the definition of  $e^x d\eta = c dt$  we have the following:

$$\begin{aligned} \frac{d\eta}{dt} &= \frac{d\eta}{dx} \frac{dx}{dt} = \frac{d\eta}{dx} H = e^{-x} c \\ \Rightarrow \frac{d\eta}{dx} &= \frac{c}{H}. \end{aligned} \quad (\text{A.3})$$

Likewise, for  $t$  we have:

$$\begin{aligned} \frac{d\eta}{dt} &= \frac{d\eta}{dx} \frac{dx}{dt} = \frac{dx}{dt} \frac{c}{H} = e^{-x} c \\ \Rightarrow \frac{dt}{dx} &= \frac{e^x}{H} = \frac{1}{H}. \end{aligned} \quad (\text{A.4})$$

## Appendix B: Sanity checks

### B.1. For $\mathcal{H}$

We start with the Hubble equation from ?? and realize that we may write any derivative of  $U$  as

$$\frac{d^n U}{dx^n} = \sum_i (-\alpha_i)^n \Omega_{i0} e^{-\alpha_i x}. \quad (\text{B.1})$$

We further have:

$$\frac{d\mathcal{H}}{dx} = \frac{H_0}{2} U^{-\frac{1}{2}} \frac{dU}{dx}, \quad (\text{B.2})$$

and

$$\begin{aligned} \frac{d^2 \mathcal{H}}{dx^2} &= \frac{d}{dx} \frac{d\mathcal{H}}{dx} \\ &= \frac{H_0}{2} \left[ \frac{dU}{dx} \left( \frac{d}{dx} U^{-\frac{1}{2}} \right) + U^{-\frac{1}{2}} \left( \frac{d}{dx} \frac{dU}{dx} \right) \right] \\ &= H_0 \left[ \frac{1}{2U^{\frac{1}{2}}} \frac{d^2 U}{dx^2} - \frac{1}{4U^{\frac{3}{2}}} \left( \frac{dU}{dx} \right)^2 \right] \end{aligned} \quad (\text{B.3})$$

Multiplying both equations with  $\mathcal{H}^{-1} = 1/(H_0 U^{\frac{1}{2}})$  yield the following:

$$\frac{1}{\mathcal{H}} \frac{d\mathcal{H}}{dx} = \frac{1}{2U} \frac{dU}{dx}, \quad (\text{B.4})$$

and

$$\begin{aligned} \frac{1}{\mathcal{H}} \frac{d^2 \mathcal{H}}{dx^2} &= \frac{1}{2U} \frac{d^2 U}{dx^2} - \frac{1}{4U^2} \left( \frac{dU}{dx} \right)^2 \\ &= \frac{1}{2U} \frac{d^2 U}{dx^2} - \left( \frac{1}{\mathcal{H}} \frac{d\mathcal{H}}{dx} \right)^2 \end{aligned} \quad (\text{B.5})$$

We now make the assumption that one of the density parameters dominate  $\Omega_i \gg \sum_{j \neq i} \Omega_j$ , enabling the following approximation:

$$U \approx \Omega_{i0} e^{-\alpha_i x}$$

$$\frac{d^n U}{dx^n} \approx (-\alpha_i)^n \Omega_{i0} e^{-\alpha_i x}, \quad (\text{B.6})$$

from which we are able to construct:

$$\frac{1}{\mathcal{H}} \frac{d\mathcal{H}}{dx} \approx \frac{-\alpha_i \Omega_{i0} e^{-\alpha_i x}}{2\Omega_{i0} e^{-\alpha_i x}} = -\frac{\alpha_i}{2}, \quad (\text{B.7})$$

and

$$\begin{aligned} \frac{1}{\mathcal{H}} \frac{d^2 \mathcal{H}}{dx^2} &\approx \frac{\alpha_i^2 \Omega_{i0} e^{-\alpha_i x}}{2\Omega_{i0} e^{-\alpha_i x}} - \left( \frac{\alpha_i}{2} \right)^2 \\ &= \frac{\alpha_i^2}{2} - \frac{\alpha_i^2}{4} = \frac{\alpha_i^2}{4} \end{aligned} \quad (\text{B.8})$$

which are quantities which should be constant in different regimes and we can easily check if our implementation of  $\mathcal{H}$  is correct, which is exactly what we sought.

### B.2. For $\eta$

**TODO: fix this** In order to test  $\eta$  we consider the definition, solve the integral and consider the same regimes as above, where one density parameter dominates:

$$\begin{aligned} \eta &= \int_{-\infty}^x \frac{cdx}{\mathcal{H}} = \frac{-2c}{\alpha_i} \int_{x=-\infty}^{x=x} \frac{d\mathcal{H}}{\mathcal{H}^2} \\ &= \frac{2c}{\alpha_i} \left( \frac{1}{\mathcal{H}(x)} - \frac{1}{\mathcal{H}(-\infty)} \right), \end{aligned} \quad (\text{B.9})$$

where we have used that:

$$\begin{aligned} \frac{d\mathcal{H}}{dx} &= -\frac{\alpha_i}{2} \mathcal{H} \\ \Rightarrow dx &= -\frac{2}{\alpha_i \mathcal{H}} d\mathcal{H}. \end{aligned} \quad (\text{B.10})$$



Since we consider regimes where one density parameter dominates, we have that  $\mathcal{H}(x) \propto \sqrt{e^{-\alpha_i x}}$ , meaning that we have:

$$\left( \frac{1}{\mathcal{H}(x)} - \frac{1}{\mathcal{H}(-\infty)} \right) \approx \begin{cases} \frac{1}{\mathcal{H}} & \alpha_i > 0 \\ -\infty & \alpha_i < 0. \end{cases} \quad (\text{B.11})$$

Combining the above yields:

$$\frac{\eta \mathcal{H}}{c} \approx \begin{cases} \frac{2}{\alpha_i} & \alpha_i > 0 \\ \infty & \alpha_i < 0. \end{cases} \quad (\text{B.12})$$

Notice the positive sign before  $\infty$ . This is due to  $\alpha_i$  now being negative.